Available online at www.sciencedirect.com

SciVerse ScienceDirect

Ceramics International 39 (2013) 1561–1566

CERAMICS INTERNATIONAL

www.elsevier.com/locate/ceramint

Charge–discharge curves and discharge capacities of $LiNi_{1-y}Co_yO_2$ synthesized from lithium carbonate and nickel and cobalt oxides

Myoung Youp Song[a,*], Ho Rim[b], Hye Ryoung Park[c], Daniel R. Mumm[d]

[a]Division of Advanced Materials Engineering, Hydrogen & Fuel Cell Research Center, Engineering Research Institute, Chonbuk National University, 567 Baekje-daero Deokjin-gu Jeonju, 561-756, Republic of Korea

[b]ASE Korea, 494 Munbal-dong Paju-si Gyeonggi-do, 413-790, Republic of Korea

[c]School of Applied Chemical Engineering, Chonnam National University, 300 Yongbong-dong Buk-gu Gwangju, 500-757, Republic of Korea

[d]Department of Chemical Engineering and Materials Science, University of California Irvine, Irvine, CA 92697-2575, USA

Received 5 July 2012; received in revised form 18 July 2012; accepted 31 July 2012
Available online 9 August 2012

Abstract

$LiNi_{1-y}Co_yO_2$ ($y=0.1$, 0.3, and 0.5) were synthesized by a solid-state reaction method at 800 °C and 850 °C using Li_2CO_3, NiO, and Co_3O_4 as the starting materials. The electrochemical properties of the synthesized $LiNi_{1-y}Co_yO_2$ were then investigated. For samples with the same composition, the particles synthesized at 850 °C were larger than those synthesized at 800 °C. The particles of all the samples synthesized at 850 °C were larger than those synthesized at 800 °C. $LiNi_{0.5}Co_{0.5}O_2$ synthesized at 850 °C had the largest first discharge capacity (159 mA h/g), followed in order by $LiNi_{0.7}Co_{0.3}O_2$ synthesized at 800 °C (158 mA h/g) and $LiNi_{0.9}Co_{0.1}O_2$ synthesized at 850 °C (151 mA h/g). $LiNi_{0.9}Co_{0.1}O_2$ synthesized at 850 °C had the best cycling performance with discharge capacities of 151 mA h/g at $n=1$ and 156 mA h/g at $n=5$.

Keywords: $LiNi_{1-y}Co_yO_2$; Solid-state reaction method; Curve of voltage vs. x in $Li_xNi_{1-y}Co_yO_2$; Discharge capacity

1. Introduction

Transition metal oxides such as $LiCoO_2$ [1–5], $LiNiO_2$ [6–13], and $LiMn_2O_4$ [14–20] have attracted attention as cathode materials for lithium secondary batteries [21]. $LiMn_2O_4$ is relatively inexpensive and environment-friendly, but its cycling performance is poor. $LiCoO_2$ has a large diffusivity and a high operating voltage, and its synthesis is easy. However, it has a disadvantage that it contains an expensive element, Co.

$LiNiO_2$ is a very promising cathode material since it has a large discharge capacity [22] and is relatively excellent economically and environmentally. However, since Li and Ni have similar sizes ($Li^+=0.72$ Å and $Ni^{2+}=0.69$ Å), the $LiNiO_2$ is practically obtained in the non-stoichiometric compositions, $Li_{1-y}Ni_{1+y}O_2$ [23,24]. The Ni^{2+} ions in the lithium planes obstruct the movement of the Li+ ions during intercalation and deintercalation [25,26].

Incorporation of $LiCoO_2$ and $LiNiO_2$ phases into $LiNi_{1-y}Co_yO_2$ compositions can overcome the shortcomings of $LiCoO_2$ and $LiNiO_2$ because the presence of cobalt stabilizes the structure in a strictly two-dimensional fashion, thus favoring good reversibility of the intercalation and deintercalation reactions [25,27–39]. Rougier et al. [25] reported that the stabilization of the two-dimensional character of the structure by cobalt substitution in $LiNiO_2$ is correlated with an increase in the cell performance, due to the decrease in the amount of extra-nickel ions in the inter-slab space which impede the lithium diffusion. Kang et al. [39] investigated the structure and electrochemical properties of the $Li_xCo_yNi_{1-y}O_2$ ($y=0.1$, 0.3, 0.5, 0.7 and 1.0) system synthesized by solid state reaction with various starting materials to optimize the characteristics and synthetic conditions of the $Li_xCo_yNi_{1-y}O_2$. The first discharge capacities of $Li_xCo_yNi_{1-y}O_2$ were 60–180 mA h/g depending on synthesis conditions.

*Corresponding author. Tel.: +82 63 270 2379; fax: +82 63 270 2386.
E-mail address: songmy@jbnu.ac.kr (M.Y. Song).

0272-8842/$ - see front matter © 2012 Elsevier Ltd and Techna Group S.r.l. All rights reserved.
http://dx.doi.org/10.1016/j.ceramint.2012.07.107

Several methods are reported to synthesize $LiNiO_2$ and $LiNi_{1-y}Co_yO_2$, such as the solid-state reaction method [40,41], the coprecipitation method [42], the sol–gel method [43], the ultrasonic spray pyrolysis method [44], the combustion method [11], and the emulsion method [45]. In this work, the solid-state reaction method, which is quite simple, was used.

Researchers used different starting materials to synthesize $LiNi_{1-y}Co_yO_2$ by the solid-state reaction method [25,27–30,32–34,38,39,46]. $LiOH \cdot H_2O$ or Li_2CO_3, NiO or $NiCO_3$, and Co_3O_4 or $CoCO_3$ have been used as starting materials by some researchers [39,46] in order to synthesize $LiNi_{1-y}Co_yO_2$ by the solid-state reaction method.

In this work, $LiNi_{1-y}Co_yO_2$ ($y=0.1$, 0.3, and 0.5) cathode materials were synthesized by a solid-state reaction method at different temperatures using Li_2CO_3, NiO, and Co_3O_4 as the sources of Li, Ni, and Co, respectively. The electrochemical properties of the synthesized samples were then investigated. The structures of the synthesized $LiNi_{1-y}Co_yO_2$ ($y=0.1$, 0.3, and 0.5) were analyzed, and the microstructures of the samples were observed. The curves of voltage vs. x in $Li_xNi_{1-y}Co_yO_2$ for first charge–discharge and intercalated and deintercalated Li quantity Δx were studied. Destruction of unstable 3b sites and phase transitions were discussed from the first and second charge–discharge curves of voltage vs. x in $Li_xNi_{0.7}Co_{0.3}O_2$.

2. Experimental

Li_2CO_3, NiO and Co_3O_4 were used as starting materials in order to synthesize $LiNi_{1-y}Co_yO_2$ by the solid-state reaction method. All the starting materials (with purity 99.9%) were purchased from Aldrich Co.

The experimental procedure for the synthesis of $LiNi_{1-y}Co_yO_2$ from Li_2CO_3, NiO, and Co_3O_4 and the characterization of the synthesized samples is given schematically in Fig. 1. The mixture of the starting materials with the compositions of $LiNi_{1-y}Co_yO_2$ ($y=0.1$, 0.3, and 0.5) was sufficiently mixed and pelletized. The pellet was then heat-treated in air at 650 °C for 20 h. It was then ground, mixed, pelletized, and calcined at 800 °C or 850 °C for 20 h. Then, this pellet was cooled at a cooling rate of 50 °C/min, ground, mixed, and pelletized again. Finally, it was calcined again at 800 °C or 850 °C for 20 h.

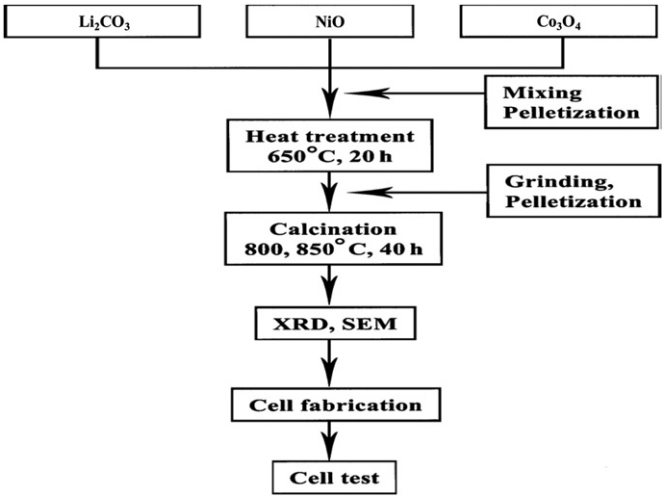

Fig. 1. Experimental procedure for the synthesis of $LiNi_{1-y}Co_yO_2$ using Li_2CO_3, NiO, and Co_3O_4 as the starting materials and the characterization of the synthesized samples.

The phase identification of the synthesized samples was carried out by X-Ray Diffraction (XRD) analysis using CuK_α radiation (Mac-Science Co., Ltd.). The scanning rate was 16°/min and the scanning range of diffraction angle (2θ) is $10° \le 2\theta \le 70°$. The morphologies of the samples were observed using a scanning electron microscope (SEM).

The electrochemical cells consisted of $LiNi_{1-y}Co_yO_2$ as a positive electrode, Li foil as a negative electrode, and electrolyte of 1 M $LiPF_6$ in a 1:1 (volume ratio) mixture of ethylene carbonate (EC) and dimethyl carbonate (DMC). A Whatman glass-fiber was used as the separator. The cells were assembled in an argon-filled dry box. To fabricate the positive electrode, 89 wt% synthesized oxide, 10 wt% acetylene black, and 1 wt% polytetrafluoroethylene (PTFE) binder were mixed in an agate mortar. By introducing Li metal, Whatman glass-fiber, positive electrode, and the electrolyte, the cell was assembled. All the electrochemical tests were performed at room temperature with a potentiostatic/galvanostatic system (Mac-Pile system, Bio-Logic Co. Ltd.). The cells were cycled at a current density of 200 $\mu A/cm^2$ in a voltage range of 3.2–4.3 V.

3. Results and discussion

Fig. 2 shows X-ray (CuK_α) diffraction patterns of (a) $LiNi_{0.9}Co_{0.1}O_2$, (b) $LiNi_{0.7}Co_{0.3}O_2$, and (c) $LiNi_{0.5}Co_{0.5}O_2$ synthesized at 850 °C for 40 h from Li_2CO_3, NiO, and Co_3O_4 as the starting materials. The XRD patterns of the $LiNi_{1-y}Co_yO_2$ ($y=0.1$, 0.3, and 0.5) powders are identified to correspond to a α-$NaFeO_2$ structure with a space group

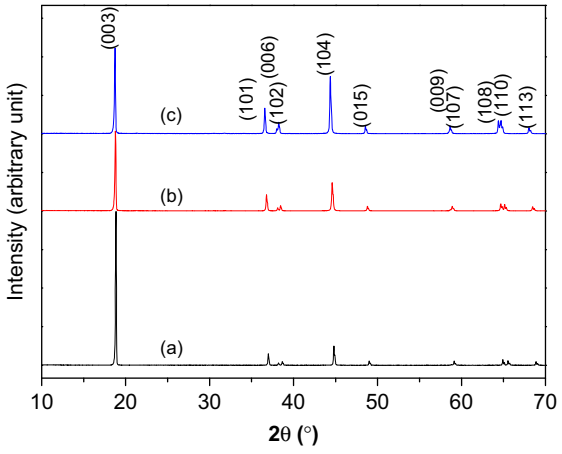

Fig. 2. X-ray (CuK_α) diffraction patterns of (a)$LiNi_{0.5}Co_{0.5}O_2$, (b) $LiNi_{0.7}Co_{0.3}O_2$, and (c) $LiNi_{0.9}Co_{0.1}O_2$ synthesized at 850 °C from Li_2CO_3, NiO, and Co_3O_4.

of $R\bar{3}m$. In Fig. 2, the relative intensity of the 003 peak compared to that of the 104 peak increases and the splitting of the (108) and (110) lines becomes clearer as the Co content increases. The fraction of each phase from the intensity ratios of the 003 and 104 peaks can be calculated since the 003 peak originates from the diffraction of only the $R\bar{3}m$ α-$NaFeO_2$ structure while the 104 peak originates from the diffractions of both the $R\bar{3}m$ α-$NaFeO_2$ and $Fm\bar{3}m$ NaCl structures. The intensity ratio of the 003 and 104 peaks, I_{003}/I_{104}, of the completely stoichiometric composition $LiNiO_2$ was reported to be about 1.3 by Morales et al. [24]. Ohzuku et al. [40] reported that the intensity ratio of the 003 and 104 peaks is a key parameter of the degree of displacement of the nickel and lithium ions. As the intensity ratio of the 003 and 104 peaks increases, the degree of displacement of the nickel and lithium ions decreases. They also reported that electroactive $LiNiO_2$ showed a clear split of the (108) and (110) lines, which appear in their XRD patterns at a diffraction angle near $2\theta=65°$.

SEM micrographs of $LiNi_{0.7}Co_{0.3}O_2$ synthesized from Li_2CO_3, NiO, and Co_3O_4 at (a) 800 °C and (b) 850 °C are shown in Fig. 3. As seen in the images, the particle size of the $LiNi_{0.7}Co_{0.3}O_2$ synthesized at 850 °C is much larger than that synthesized at 800 °C. At each temperature, the size of the particles decreased slightly as the Co content (y) increased from 0.1 to 0.3 and then grew as y increased from 0.3 to 0.5, showing that, roughly speaking, the size of the particles decreased as the Co content increased. The synthesis and thus the formation of $LiCoO_2$ are known to be easier than those of $LiNiO_2$. This may lead to the larger size of $LiNi_{1-y}Co_yO_2$ particles as the Co content increases. For samples with the same composition, the particles synthesized at 850 °C were larger than those synthesized at 800 °C. The particles of all the samples synthesized at 850 °C were larger than those synthesized at 800 °C.

The curves of the voltage vs. x in $Li_xNi_{0.7}Co_{0.3}O_2$ at a current density of 200 μA/cm^2 for the first charge–discharge of $LiNi_{0.7}Co_{0.3}O_2$ synthesized at (a) 800 °C and (b) 850 °C are shown in Fig. 4. Polarization is a change in the potentials for deintercalation and intercalation of lithium atoms. $LiNi_{0.7}Co_{0.3}O_2$ synthesized at 800 °C exhibits a smaller polarization than $LiNi_{0.7}Co_{0.3}O_2$ synthesized at 850 °C. $LiNi_{0.7}Co_{0.3}O_2$ synthesized at 800 °C has a larger discharge capacity than $LiNi_{0.7}Co_{0.3}O_2$ synthesized at 850 °C.

Fig. 5 presents the curves of the voltage vs. x in $Li_xNi_{1-y}Co_yO_2$ for the first and second charge–discharges of (a) $LiNi_{0.7}Co_{0.3}O_2$ synthesized at 800 °C and (b) $LiNi_{0.5}Co_{0.5}O_2$ synthesized at 850 °C. The value of Δx for the first discharge is very close to that for the second discharge. The values of Δx in the charges and discharges of $LiNi_{0.5}Co_{0.5}O_2$ synthesized at 850 °C are slightly larger than those of $LiNi_{0.7}Co_{0.3}O_2$ synthesized at 800 °C.

The first charge capacities at a current density of 200 μA/cm^2 in the voltage range of 3.0–4.3 V for $LiNi_{1-y}Co_yO_2$ synthesized at 800 °C and 850 °C are shown in Fig. 6. $LiNi_{0.5}Co_{0.5}O_2$ synthesized at 850 °C has the largest first discharge capacity, followed in order by $LiNi_{0.7}Co_{0.3}O_2$ synthesized at 800 °C, $LiNi_{0.9}Co_{0.1}O_2$ synthesized at 850 °C, $LiNi_{0.5}Co_{0.5}O_2$ synthesized at 800 °C, $LiNi_{0.9}Co_{0.1}O_2$ synthesized at 800 °C, and $LiNi_{0.7}Co_{0.3}O_2$ synthesized at 850 °C.

Variations of the discharge capacity with number of cycles (n) for $LiNi_{1-y}Co_yO_2$ synthesized at 800 °C: (a) $y=0.5$ and (b) $y=0.3$, and at 850 °C: (c) $y=0.5$, (d) $y=0.3$, and (e) $y=0.1$ are shown in Fig. 7. $LiNi_{0.5}Co_{0.5}O_2$ synthesized at 850 °C (159 mA h/g) had the largest first discharge capacity, followed in order by $LiNi_{0.7}Co_{0.3}O_2$ synthesized at 800 °C (158 mA h/g) and $LiNi_{0.9}Co_{0.1}O_2$ synthesized at 850 °C (151 mA h/g). $LiNi_{0.9}Co_{0.1}O_2$ synthesized at 850 °C has the best cycling performance (discharge

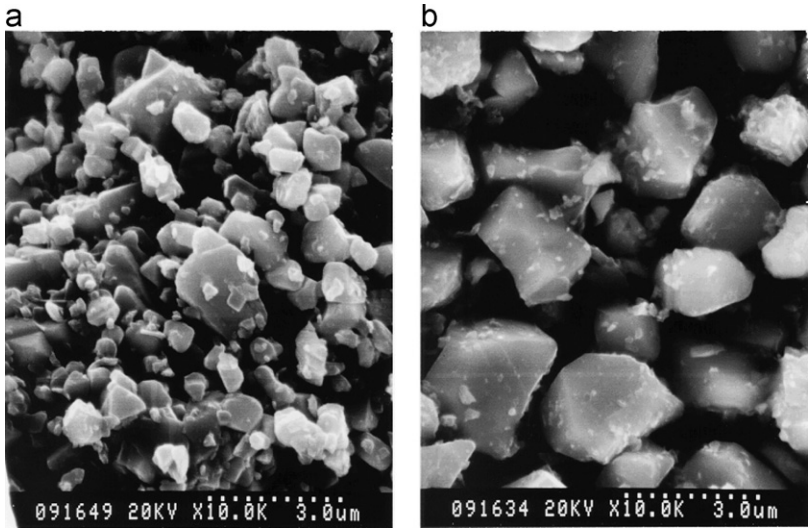

Fig. 3. SEM micrographs of $LiNi_{0.7}Co_{0.3}O_2$ synthesized from Li_2CO_3, NiO, and Co_3O_4 at (a) 800 °C and (b) 850 °C.

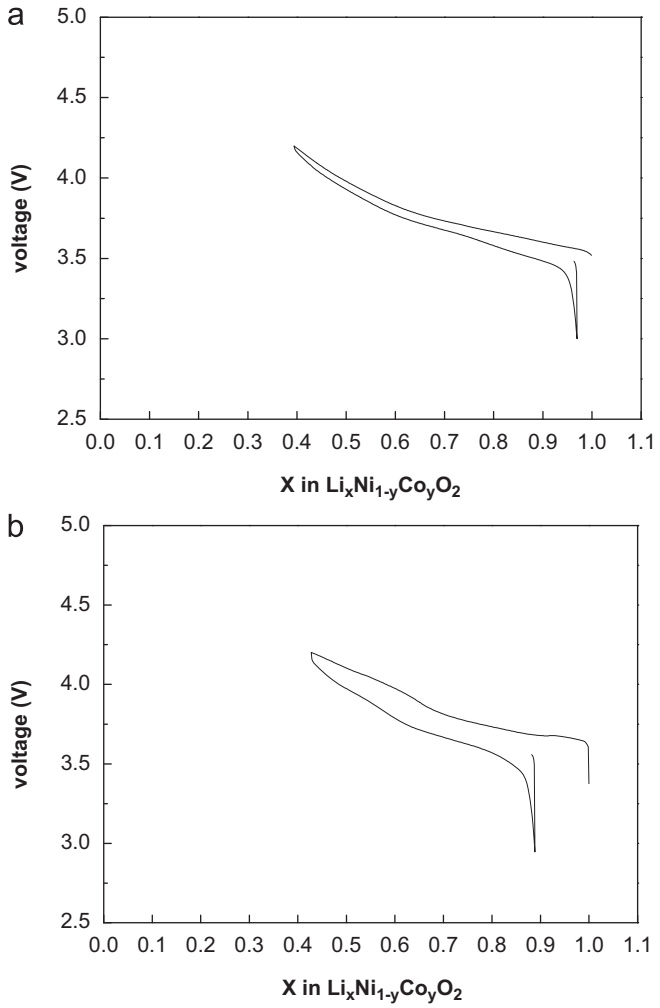

Fig. 4. Curves of the voltage vs. x in $Li_xNi_{0.7}Co_{0.3}O_2$ at a current density of 200 μA/cm² for the first charge–discharge of $LiNi_{0.7}Co_{0.3}O_2$ synthesized from Li_2CO_3, NiO, and Co_3O_4 at (a) 800 °C and (b) 850 °C.

capacity degradation rate of 0.8 mA h/g/cycle) with discharge capacities of 151 mA h/g at $n=1$ and 156 mA h/g at $n=5$, followed by $LiNi_{0.7}Co_{0.3}O_2$ synthesized at 850 °C (discharge capacity degradation rate of 2.9 mA h/g/cycle). The other samples have similar cycling performances.

The curves of the voltage vs. x in $Li_xNi_{1-y}Co_yO_2$ at a current density of 200 μA/cm² for the first charge–discharge of $LiNi_{1-y}Co_yO_2$ in Fig. 4 show that, as compared with the quantity of the deintercalated Li ions by the first charging, that of the intercalated Li ions by the first discharging is much smaller, which is revealed by the difference in Δx of the first charge and discharge curves, for all the samples. The lengths of plateaus in the charge and discharge curves are proportional to charge and discharge capacities. During the first charging, Li ions deintercalate not only from stable 3b sites but also from unstable 3b sites. After deintercalation from unstable 3b sites, the unstable 3b sites will be destroyed. This is considered to lead to smaller quantity of the intercalated Li ions by the first discharging than that of the deintercalated Li ions by the first charging.

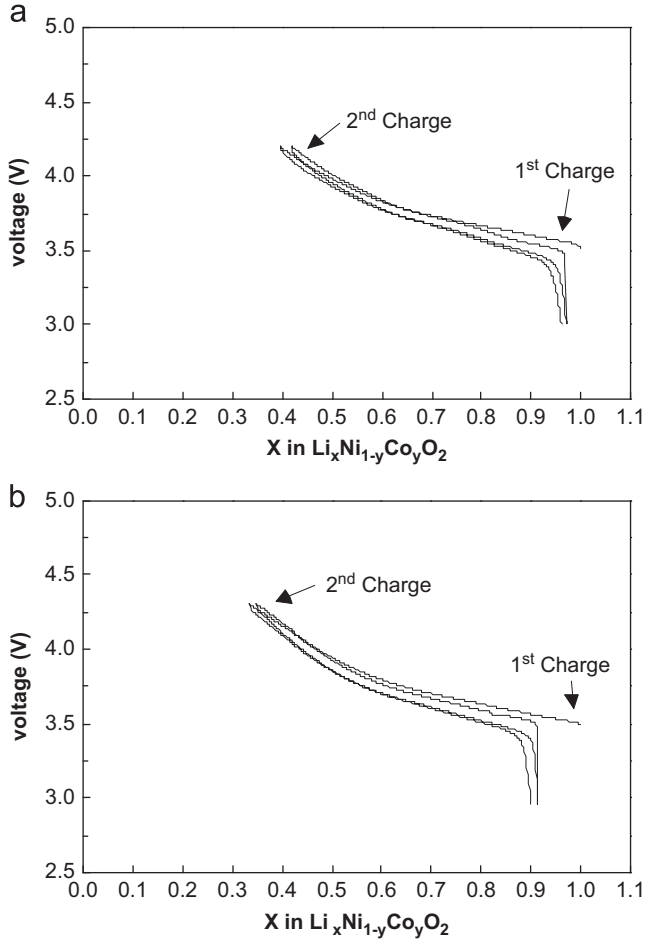

Fig. 5. Curves of the voltage vs. x in $Li_xNi_{1-y}Co_yO_2$ for the first and second charge–discharges of (a) $LiNi_{0.7}Co_{0.3}O_2$ synthesized at 800 °C and (b) $LiNi_{0.5}Co_{0.5}O_2$ synthesized at 850 °C.

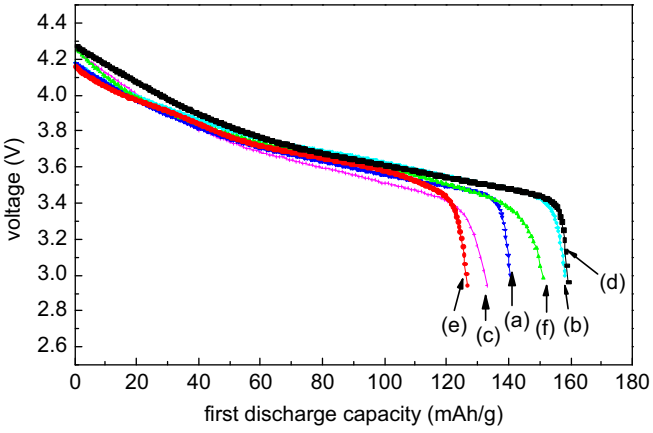

Fig. 6. First charge capacities at a current density of 200 μA/cm² in the voltage range of 3.0–4.3 V for $LiNi_{1-y}Co_yO_2$ synthesized at 800 °C: (a) $y=0.5$, (b) $y=0.3$, and (c) $y=0.1$, and at 850 °C: (d) $y=0.5$, (e) $y=0.3$, and (f) $y=0.1$.

The curves of the voltage vs. x in $Li_xNi_{1-y}Co_yO_2$ for the first and second charge–discharges of $LiNi_{0.7}Co_{0.3}O_2$ synthesized at 800 °C and $LiNi_{0.5}Co_{0.5}O_2$ synthesized

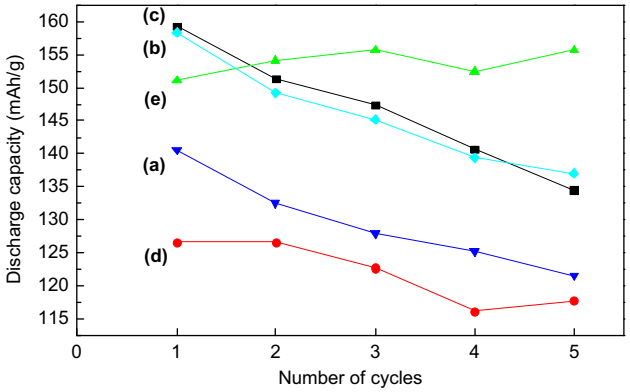

Fig. 7. Variations of the discharge capacity with number of cycles (n) for $LiNi_{1-y}Co_yO_2$ synthesized at 800 °C: (a) $y=0.5$ and (b) $y=0.3$, and at 850 °C: (c) $y=0.5$, (d) $y=0.3$, and (e) $y=0.1$.

850 °C in Fig. 5 show that the differences in Δx of the second charge and discharge curves are smaller than those of the first charge and discharge curves. This shows that destruction of unstable 3b sites occurs less severely at the second cycle than at the first cycle.

In the curves of the voltage vs. x in $Li_xNi_{1-y}Co_yO_2$ for the first and second charge–discharges of $LiNi_{0.7}Co_{0.3}O_2$ synthesized at 800 °C and $LiNi_{0.5}Co_{0.5}O_2$ synthesized 850 °C in Fig. 5, the charge–discharge curves exhibit quite long plateaus, where two phases co-exist [47]. Arai et al. [48] reported that, during charging and discharging, $LiNiO_2$ goes through three phase transitions; phase transitions from hexagonal structure (H1) to monoclinic structure (M), from monoclinic structure (M) to hexagonal structure (H2), and from hexagonal structure (H2) to hexagonal structure (H3) or vice versa. Ohzuku et al. [40] reported that, during charging and discharging, $LiNiO_2$ goes through four phase transitions; phase transitions from H1 to M, from M to H2, from H2 to hexagonal structures H2+H3, and from H2+H3 to H3 or vice versa. Song et al. [49] reported that $-dx/|dV|$ vs. V curves of $LiNi_{1-y}Ti_yO_2$ ($y=0.012$ and 0.025) for charging and discharging showed four peaks, revealing the four phase transitions from H1 to M, from M to H2, from H2 to H2+H3, and from H2+H3 to H3 or vice versa.

4. Conclusions

The XRD patterns of the synthesized $LiNi_{1-y}Co_yO_2$ ($y=0.1$, 0.3, and 0.5) powders were identified to correspond to a α-$NaFeO_2$ structure with a space group of $R\bar{3}m$. For samples with the same composition, the particles synthesized at 850 °C were larger than those synthesized at 800 °C. The particles of all the samples synthesized at 850 °C were larger than those synthesized at 800 °C. $LiNi_{0.5}Co_{0.5}O_2$ synthesized at 850 °C (159 mA h/g) had the largest first discharge capacity, followed in order by $LiNi_{0.7}Co_{0.3}O_2$ synthesized at 800 °C (158 mA h/g) and $LiNi_{0.9}Co_{0.1}O_2$ synthesized at 850 °C (151 mA h/g). $LiNi_{0.9}Co_{0.1}O_2$ synthesized at 850 °C had the best cycling performance with discharge capacities of 151 mA h/g at $n=1$ and 156 mA h/g at $n=5$. The curves of the voltage vs. x in $Li_xNi_{1-y}Co_yO_2$ for the first charge–discharge of $LiNi_{1-y}Co_yO_2$ showed that after deintercalation from unstable 3b sites, the unstable 3b sites will be destroyed, leading to a smaller quantity of the intercalated Li ions by the first discharging than that of the deintercalated Li ions by the first charging.

References

[1] K. Ozawa, Lithium-ion rechargeable batteries with $LiCoO_2$ and carbon electrodes: the $LiCoO_2$/C system, Solid State Ionics 69 (1994) 212–221.
[2] R. Alcántara, P. Lavela, J.L. Tirado, R. Stoyanova, E. Zhecheva, Structure and electrochemical properties of boron-doped $LiCoO_2$, Journal of Solid State Chemistry 134 (1997) 265–273.
[3] Z.S. Peng, C.R. Wan, C.Y. Jiang, Synthesis by sol–gel process and characterization of $LiCoO_2$ cathode materials, Journal of Power Sources 72 (1998) 215–220.
[4] W.D. Yang, C.Y. Hsieh, H.J. Chuang, Y.S. Chen, Preparation and characterization of nanometric-sized $LiCoO_2$ cathode materials for lithium batteries by a novel sol–gel method, Ceramics International 36 (1) (2010) 135–140.
[5] S.K. Kim, D.H. Yang, J.S. Sohn, Y.C. Jung, Resynthesis of $LiCo_{1-x}Mn_xO_2$ as a cathode material for lithium secondary batteries, Metals and Materials International 18 (2) (2012) 321–326.
[6] J.R. Dahn, U. von Sacken, C.A. Michal, Structure and electrochemistry of $Li_{1\pm y}NiO_2$ and a new Li_2NiO_2 phase with the $Ni(OH)_2$ structure, Solid State Ionics 44 (1990) 87–97.
[7] J.R. Dahn, U. von Sacken, M.W. Juzkow, H. Al-Janaby, Rechargeable $LiNiO_2$/carbon cells, Journal of the Electrochemical Society 138 (1991) 2207–2212.
[8] H.U. Kim, D.R. Mumm, H.R. Park, M.Y. Song, Synthesis by a simple combustion method and electrochemical properties of $LiCo_{1/3}Ni_{1/3}Mn_{1/3}O_2$, Electronic Materials Letters 6 (3) (2010) 91–95.
[9] S.H. Ju, J.H. Kim, Y.C. Kang, Electrochemical properties of $LiNi_{0.8}Co_{0.2-x}Al_xO_2$ ($0<x<0.1$) cathode particles prepared by spray pyrolysis from the spray solutions with and without organic additives, Metals and Materials International 16 (2) (2010) 299–303.
[10] D.H. Kim, Y.U. Jeong, D.H. Kim, Y.U. Jeong, Crystal structures and electrochemical properties of $LiNi_{1-x}Mg_xO_2$ ($0<x<0.1$) for cathode materials of secondary lithium batteries, Korean Journal of Metals and Materials 48 (3) (2010) 262–267.
[11] S.N. Kwon, J.H. Song, D.R. Mumm, Effects of cathode fabrication conditions and cycling on the electrochemical performance of $LiNiO_2$ synthesized by combustion and calcination, Ceramics International 37 (5) (2011) 1543–1548.
[12] M.Y. Song, C.K. Park, H.R. Park, D.R. Mumm, Variations in the electrochemical properties of metallic elements-substituted $LiNiO_2$ cathodes with preparation and cathode fabrication conditions, Electronic Materials Letters 8 (1) (2012) 37–42.
[13] M.Y. Song, D.R. Mumm, C.K. Park, H.R. Park, Cycling performances of $LiNi_{1-y}M_yO_2$ (M=Ni, Ga, Al and/or Ti) synthesized by wet milling and solid-state method, Metals and Materials International 18(3) (2012) 465–472.
[14] J.M. Tarascon, E. Wang, F.K. Shokoohi, W.R. Mckinnon, S. Colson, The spinel phase of $LiMn_2O_4$ as a cathode in secondary lithium cells, Journal of the Electrochemical Society 138 (1991) 2859–2864.
[15] A.R. Armstrong, P.G. Bruce, Synthesis of layered $LiMnO_2$ as an electrode for rechargeable lithium batteries, Nature 381 (1996) 499–500.
[16] M.Y. Song, D.S. Ahn, On the capacity deterioration of spinel phase $LiMn_2O_4$ with cycling around 4 V, Solid State Ionics 112 (1998) 21–24.

[17] M.Y. Song, D.S. Ahn, H.R. Park, Capacity fading of spinel phase $LiMn_2O_4$ with cycling, Journal of Power Sources 83 (1999) 57–60.
[18] D.S. Ahn, M.Y. Song, Variations of the electrochemica properties of $LiMn_2O_4$ with synthesis conditions, Journal of the Electrochemical Society 147 (3) (2000) 874–879.
[19] H.J. Guo, Q.H. Li, X.H. Li, Z.X. Wang, W.J. Peng, Novel synthesis of $LiMn_2O_4$ with large tap density by oxidation of manganese powder, Energy Conversion and Management 52 (4) (2011) 2009–2014.
[20] C. Wan, M. Cheng, D. Wu, Synthesis of spherical spinel $LiMn_2O_4$ with commercial manganese carbonate, Powder Technology 210 (1) (2011) 47–51.
[21] J.W. Park, J.H. Yu, K.W. Kim, H.S. Ryu, J.H. Ahn, C.S. Jin, K.H. Shin, Y.C. Kim, H.J. Ahn, Surface morphology changes of lithium/sulfur battery using multi-walled carbon nanotube added sulfur electrode during cyclings, Korean Journal of Metals and Materials 49 (2) (2011) 174–179.
[22] Y. Nishida, K. Nakane, T. Satoh, Synthesis and properties of gallium-doped $LiNiO_2$ as the cathode material for lithium secondary batteries, Journal of Power Sources 68 (1997) 561–564.
[23] P. Barboux, J.M. Tarascon, F.K. Shokoohi, The use of acetates as precursors for the low-temperature synthesis of $LiMn_2O_4$ and $LiCoO_2$ intercalation compounds, Journal of Solid State Chemistry 94 (1991) 185–196.
[24] J. Morales, C. Perez-Vicente, J.L. Tirado, Cation distribution and chemical deintercalation of $Li_{1-x}Ni_{1+x}O_2$, Materials Research Bulletin 25 (1990) 623–630.
[25] A. Rougier, I. Saadoune, P. Gravereau, P. Willmann, C. Delmas, Effect of cobalt substitution on cationic distribution in $LiNi_{1-y}Co_yO_2$ electrode materials, Solid State Ionics 90 (1996) 83–90.
[26] B.J. Neudecker, R.A. Zuhr, B.S. Kwak, J.B. Bates, J.D. Robertson, Lithium manganese nickel oxides $Li_x(Mn_yNi_{1-y})_{2-x}O_2$, Journal of the Electrochemical Society 145 (1998) 4148–4157.
[27] C. Delmas, I. Saadoune, Electrochemical and physical properties of the $Li_xNi_{1-y}Co_yO_2$ phases, Solid State Ionics 53–56 (1992) 370–375.
[28] E. Zhecheva, R. Stoyanova, Stabilization of the layered crystal structure of $LiNiO_2$ by Co-substitution, Solid State Ionics 66 (1993) 143–149.
[29] C. Delmas, I. Saadoune, A. Rougier, The cycling properties of the $Li_xNi_{1-y}Co_yO_2$ electrode, Journal of Power Sources 43,44 (1993) 595–602.
[30] A. Ueda, T. Ohzuku, Solid-state redox reactions of $LiNi_{1/2}Co_{1/2}O_2$ ($R\bar{3}m$) for 4 V secondary lithium cells, Journal of the Electrochemical Society 141 (1994) 2010–2014.
[31] M. Menetrier, A. Rougier, C. Delmas, Cobalt segregation in the $LiNi_{1-y}Co_yO_2$ solid solution: a preliminary ^7Li NMR study, Solid State Communications 90 (1994) 439–442.
[32] R. Alcantara, J. Morales, J.L. Tirado, R. Stoyanova, E. Zhecheva, Structure and electrochemical properties of $Li_{1-x}(Ni_yCo_{1-y})_{1+x}O_2$. Effect of chemical delithiation at 0 °C, Journal of the Electrochemical Society 142 (1995) 3997–4005.
[33] B. Banov, J. Bourilkov, M. Mladenov, Cobalt stabilized layered lithium–nickel oxides, cathodes in lithium rechargeable cells, Journal of Power Sources 54 (1995) 268–270.
[34] Y.M. Choi, S.I. Pyun, S.I. Moon, Effects of cation mixing on the electrochemical lithium intercalation reaction into porous $Li_{1-\delta}Ni_{1-y}Co_yO_2$ electrodes, Solid State Ionics 89 (1996) 43–52.
[35] S.J. Lee, J.K. Lee, D.W. Kim, H.K. Baik, S.M. Lee, Fabrication of thin film $LiCo_{0.5}Ni_{0.5}O_2$ cathode for Li rechargeable microbattery, Journal of the Electrochemical Society 143 (1996) L268–L270.
[36] D. Caurant, N. Baffier, B. Garcia, J.P. Pereira-Ramos, Synthesis by a soft chemistry route and characterization of $LiNi_xCo_{1-x}O_2$ ($0 < x < 1$) cathode materials, Solid State Ionics 91 (1996) 45–54.
[37] K. Amine, H. Yasuda, Y. Fujita, New process for low temperature preparation of $LiNi_{1-x}Co_xO_2$ cathode material for lithium cells, Annales de Chimie Science des Matériaux 23 (1998) 37–42.
[38] C.C. Chang, N. Scarr, P.N. Kumta, Synthesis and electrochemical characterization of $LiMO_2$ (M = Ni, $Ni_{0.75}Co_{0.25}$) for rechargeable lithium ion batteries, Solid State Ionics 112 (1998) 329–344.
[39] S.G. Kang, K.S. Ryu, S.H. Chang, S.C. Park, The novel synthetic route to $LiCo_yNi_{1-y}O_2$ as a cathode material in lithium secondary batteries, Bulletin of the Korean Chemical Society 22 (12) (2001) 1328–1332.
[40] T. Ohzuku, A. Ueda, M. Nagayama, Electrochemistry and structural chemistry of $LiNiO_2$ ($R\bar{3}m$) for 4 V secondary lithium cells, Journal of the Electrochemical Society 140 (1993) 1862–1870.
[41] Z. Lu, X. Huang, H. Haung, L. Chen, J. Schoonman, The phase transition and optimal synthesis temperature of $LiNiO_2$, Solid State Ionics 120 (1999) 103–107.
[42] M. Guilmard, A. Rougier, M. Grune, L. Croguennec, C. Delmas, Effects of aluminum on the structural and electrochemical properties of $LiNiO_2$, Journal of Power Sources 115 (2003) 305–314.
[43] B.J. Hwang, R. Santhanam, C.H. Chen, Effect of synthesis conditions on electrochemical properties of $LiCo_yNi_{1-y}O_2$ cathode for lithium rechargeable batteries, Journal of Power Sources 114 (2003) 244–252.
[44] S.H. Park, C.S. Yoon, S.G. Kang, H.S. Kim, S.I. Moon, Y.K. Sun, Synthesis and structural characterization of layered Li $[Ni_{1/3}Co_{1/3}Mn_{1/3}]O_2$ cathode materials by the ultrasonic spray pyrolysis method, Electrochimica Acta 49 (2004) 557–563.
[45] B.H. Kim, J.H. Kim, I.H. Kwon, M.Y. Song, Electrochemical properties of $LiNiO_2$ cathode material synthesized by the emulsion method, Ceramics International 33 (2007) 837–841.
[46] M.Y. Song, H. Rim, E. Bang, Electrochemical properties of cathode materials $LiNi_{1-y}Co_yO_2$ synthesized using various starting materials, Journal of Applied Electrochemistry 34 (2004) 383–389.
[47] W. Li, J.N. Reimers, J.R. Dahn, In situ x-ray diffraction and electrochemical studies of $Li_{1-x}NiO_2$, Solid State Ionics 67 (1993) 123–130.
[48] H. Arai, S. Okada, H. Ohtsuka, M. Ichimura, J. Yamaki, Characterization and cathode performance of $Li_{1-x}Ni_{1+x}O_2$ prepared with the excess lithium method, Solid State Ionics 80 (1995) 261–269.
[49] M.Y. Song, D.S. Lee, H.R. Park, Electrochemical properties of $LiNi_{1-y}Ti_yO_2$ and $LiNi_{0.975}M_{0.025}O_2$ (M = Zn, Al, and Ti) synthesized by the solid-state reaction method, Materials Research Bulletin 47 (2012) 1021–1027.